Available online at www.sciencedirect.com
SCIENCE DIRECT®
ELSEVIER
Journal of Constructional Steel Research 61 (2005) 1135–1146
JOURNAL OF CONSTRUCTIONAL STEEL RESEARCH
www.elsevier.com/locate/jcsr

Analysis of steel storage rack columns

A.M.S. Freitas*, M.S.R. Freitas, F.T. Souza

Department of Civil Engineering, School of Mines, Federal University of Ouro Preto, Campus Morro do Cruzeiro, 35400-000 Ouro Preto, MG, Brazil

Abstract

Storage rack systems are structures composed of cold-formed steel structural members that are used as columns, beams and bracing. The rack columns present peculiar features in their design because they have perforations to facilitate assemblage of the system, which makes them more difficult to analyze by cold-formed steel structures design codes. There are several design codes proposed by the manufacturers associations, as the specifications of Rack Manufacturers Institute (RMI), applied in the USA along with the specification of the American Iron and Steel Institute (AISI). These codes propose experimental stub columns tests for the determination of their resistance. In this work, the commercial software, ANSYS, is used for material and geometric non-linear analysis of these columns, and the results are compared with experimental data obtained by stub column tests, for a typical section of racks manufactured in Brazil.

Keywords: Cold-formed elements; Thin-walled perforated members; Stub columns; Finite element analysis

1. Introduction

Cold-formed steel sections have become usual in many kinds of structures, and consequently much research has been done to understand their behaviour and to develop design procedures. Among these structures, there are the storage systems, usually called racks, widely used throughout the world for storing materials in distribution companies. These systems provide high storage density, allowing the storage of a great amount of products in reduced areas, due to their vertical character. Besides, they also allow great

* Corresponding author. Tel.: +55 31 3559 1554; fax: +55 31 3559 1548.
E-mail address: arlene@em.ufop.br (A.M.S. Freitas).

0143-974X/$ - see front matter © 2005 Elsevier Ltd. All rights reserved.
doi:10.1016/j.jcsr.2005.02.004

Fig. 1. Steel storage systems in operation [1].

accessibility to the stored materials. Many companies are using these systems to store their product in large scale.

There are several commercial models that fit to the conditions demanded for each product to be stored in the available room. These models vary from simple shelves to automated structures of more than 30 m height. Among these several models, it is worth mentioning the Pallet and Drive-in Systems. The Pallet rack is the most common storage rack used in Brazil. The Drive-in model presents peculiar structural concepts: the absence of transversal beams to allow trucks to move inside the structure and the presence of perforations on the columns to facilitate assemblage. Fig. 1 shows a Pallet and a Drive-in rack in operation [1].

The Brazilian Association of Handling and Logistic has introduced some recommendations for designing rack systems that, in the future, will be used in a Brazilian code. This work presents an analysis of typical columns of commercial Brazilian racks, using the commercial finite element software ANSYS [2]. The results are compared with experimental data, based on prescriptions of RMI [3] and from previous work (Oliveira [4]). The influence of the perforations and geometric imperfections on the resistance of the columns is also assessed.

2. The rack column

The analyzed column is made of cold-formed steel [5], where the cross-section shape is a thin-walled “rack”. One of these cross sections and the nomenclature used for the identification of its parts are presented in Fig. 2. It has as particularity rear flanges that allow fitting the braces, making it easier to assemble the structure.

The main characteristic of the column, however, is the existence of perforations along its height that allows fitting the connections of braces and other structural elements. These perforations influence the structural behaviour of the column and, therefore, should be taken into account in the project analyses. To quantify the influence of the perforations

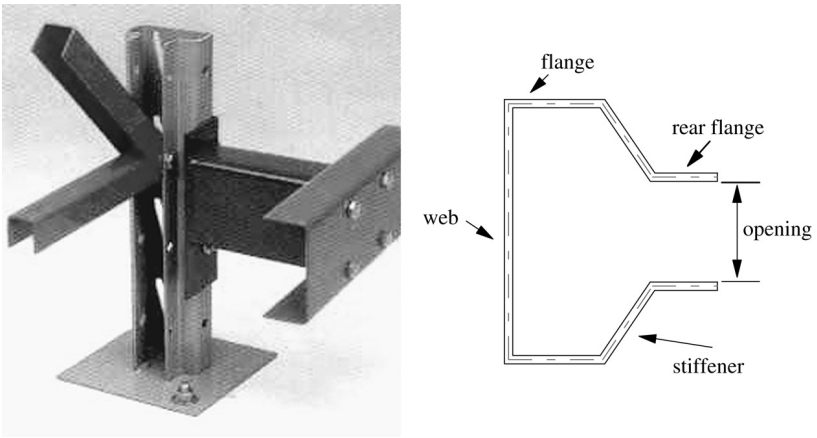

Fig. 2. Connections in the column (Águia), "Rack" cross-section type and nomenclature.

on the load capacity of the columns, experimental and numerical methods are used. RMI presents prescriptions for this evaluation by means of experimental procedures that will be presented in Section 3. In this paper, experimental and numerical procedures are used in this evaluation.

3. Design concept

The use of thin-walled sections can result in specific design problems due to the failure modes such as local buckling and distortional buckling [6]. The rack sections usually contain perforations and imperfections that decrease the resistance of these members. The design rules intended for these members use minimum geometric properties and experimental results to predict the behaviour of the structure.

For the evaluation of the load capacity of the column by the RMI specification it is necessary to carry out a stub column compression test of a typical rack cross section. This test uses a specimen that has its dimensions defined in a way to eliminate overall column buckling effects and to minimize the end effects during loading [7]. Fig. 3 presents a general view of the specimen and its dimensions used in the experimental program.

The specimen is submitted to a compression load applied in the gravity center of the minimum net area of the cross section, $CG_{\min}$. The load is applied through a Universal Testing Machine, and transmitted by rigid plates to the column, without any perforations in the ends, as shown in Fig. 3. Fig. 4 shows a schematic view of the stub column test. Through this test the ultimate strength of the column is obtained. The equations below, proposed by Peköz [8] and presented by the RMI specification, are used for computing the nominal member capacity of the column.

$$P_n = A_e F_n \tag{1}$$

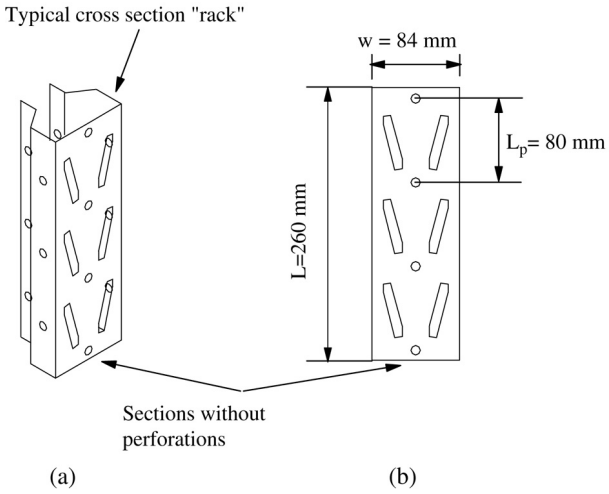

Fig. 3. General view of the specimens: (a) Perspective; (b) View with the dimensions of the maximum width, w, distance between perforations, L_p, and total length, L.

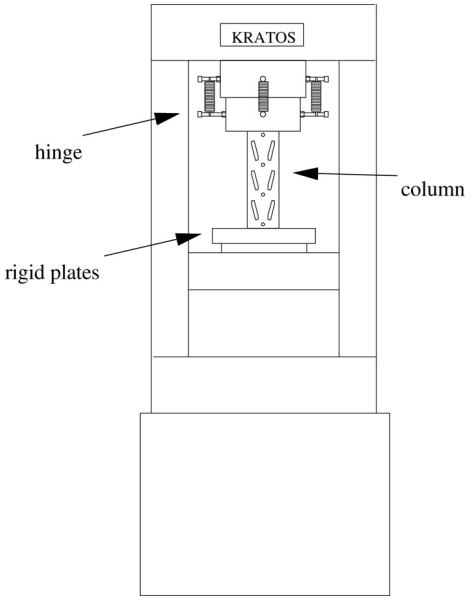

Fig. 4. Stub column test.

where P_n is the nominal axial load, F_n is the nominal buckling critical stress [7] and A_e is the effective area of the cross section, given by Eq. (2).

$$A_e = \left[1 - (1 - Q)\left(\frac{F_n}{f_{ya}}\right)^Q\right] A_{netmin} \tag{2}$$

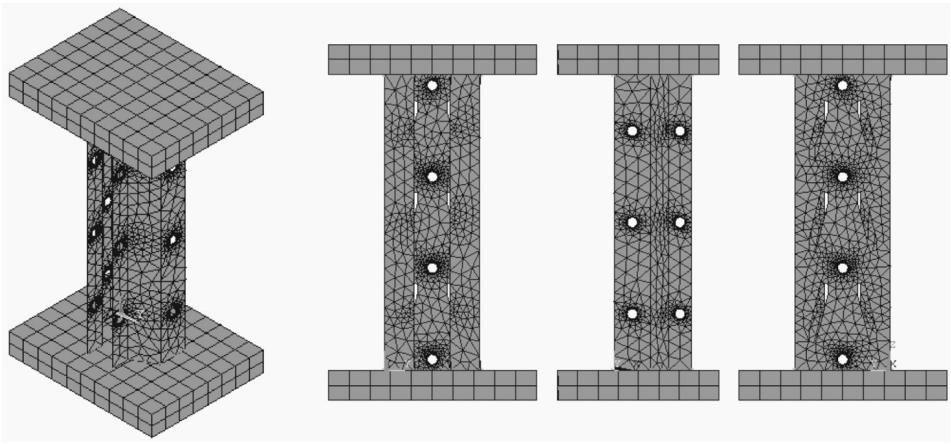

Fig. 5. Finite element meshes: (a) Isometric view; (b) Frontal view; (c) Flanges view; (d) Web view.

where f_{ya} is the actual yield stress of the column material by test, A_{netmin} is the minimum cross-sectional area and Q is the form reduction factor, given by Eq. (3).

$$Q = \frac{P_{ua}}{f_{ya} A_{netmin}} \tag{3}$$

where P_{ua} is the ultimate compressive strength of stub column by test.

The form factor Q comprises the effects of local buckling and the interaction with the perforations. The maximum value of Q is the unit to take into account the effect described earlier. The reduced area caused by the perforations is also considered by using the term A_{netmin} in Eq. (2). The distortional buckling mode could control the critical stress in rack sections, but it is not considered in the RMI prescriptions.

The use of laboratory tests to evaluate the influence of the perforations raises costs of design. Thus, using alternatives for validating procedures that may well represent experimental results is important and it is the focus of this research through the use of the finite element method.

4. Finite element analysis

This item presents the constructional procedures of the finite element model for the proposed non-linear analysis using the software ANSYS. The prototype of the cold-formed steel column and its cross section presented in Fig. 2 can be simulated using a shell element. To consider the shape of the perforations in the mesh, a triangular mesh was used, with automatic adjust and fine rate, generating small elements that can exactly contour the perforations. Fig. 5 presents the finite element meshes generated in ANSYS.

Rigid plates were included in the analysis to simulate the test machine load transmission plates. Their Young's modulus was considered to be 20 000 GPa, so as to minimize the deformations in the plates as in actual cases. The rigid plates were simulated using a

Table 1
Finite elements used in the analysis

Element	SHELL43	SOLID45	CONTAC49
Description of element	Plastic Shell element	3-D structural solid element	Contact between column and plates
Number of nodes	4	8	5
Degrees of freedom	x, y and z translational and rotational displacements	x, y and z translational displacements	x, y and z translational displacements
Use in the model	Column	Reaction plates	Contact between column and plates

solid element and they were assumed to have free displacement along the axial direction, and restrained displacement along the cross-section directions. These boundary conditions represent well the test conditions.

The simulation of friction between the rigid plates and the column was achieved by using a contact element proper to link solid and shell elements. A friction coefficient of 0.33 was considered.

The techniques used to manufacture cold-formed steel section produce residual stresses and substantial changes on the mechanical properties. The residual stress distribution is not constant around the section [9]. Due to perforations, tensile coupons used in the tests were extracted in the stiffener zone, so this region indicates the stress–strain behaviour of the steel.

Two different cases were simulated. In the first the material properties, represented by the stress–strain curve of the steel, were obtained from experimental data [10]. These values were introduced in the numerical analysis by a bi-linear diagram. In this diagram, Young's modulus of elasticity (E) is 205 GPa, yield stress (f_y) is 320.23 MPa and ultimate stress (f_u) is 432.5 MPa. In the second case nominal elasticity properties were considered, this is, f_y and f_u equal to 250 MPa and 400 MPa, respectively. It is important to point out that the distribution of residual stresses was not used in the analysis and the tensile coupons were taken from the stiffener wall (Fig. 2).

Firstly the column was simulated considering the nominal dimensions of the specimen. In that stage, the friction was not considered between the column and the plates [11]. Later the non-linear behaviour was introduced by considering friction and the geometric imperfections measured in the actual specimens, in order to simulate the real conditions of the tests [12].

The shell, solid and contact elements used for the simulation are presented in Table 1.

5. Results

5.1. Experimental results

Ultimate compressive strength was evaluated. The experimental program consisted of 4 specimens tested by the "stub column test", described in Section 3. Fig. 6 shows

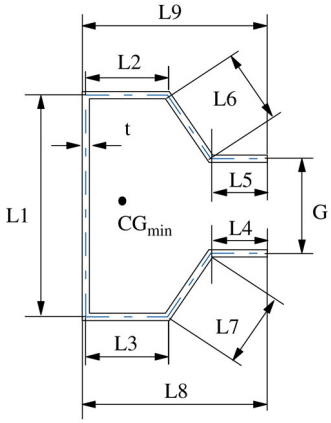

	Average dimension
L1	81.14 mm
L2	32.03 mm
L3	31.95 mm
L4	21.56 mm
L5	18.85 mm
L6	24.34 mm
L7	25.36 mm
L8	66.80 mm
L9	67.12 mm
G	41.80 mm
t	2.65 mm
A_{netmin}	478.192 mm^2
CG_{min}	21.605 mm

Fig. 6. Average dimensions of cross section.

Table 2
Results of P_{uexp} and P_{ua}

Specimen	P_{uexp} (kN)
CCMAX-1	144.207
CCMAX-2	136.604
CCMAX-3	140.773
CCMAX-4	137.340
P_{ua} (kN)	139.731

the average actual dimensions of the cross sections tested and the gravity center of the minimum net area, CG_{min}. Table 2 shows the experimental results of the ultimate axial load, P_{ua}. As prescribed by the stub column test only the ultimate compressive load was measured.

By using Eq. (3) and the experimental results the form factor Q was determined ($Q = 0.914$).

5.2. Load capacity

The perforation influence in the load capacity was simulated using different cross-sectional areas. In the numerical simulation of the column, the ultimate load was assessed for several situations, as given:

- Actual cross section of the column, considering the perforations, with nominal dimensions called *nominal column*.
- Actual cross section of the column, considering the perforations, with actual dimensions called *actual column*.
- Full cross section of the column, without perforations, and with nominal dimensions called *gross column*.

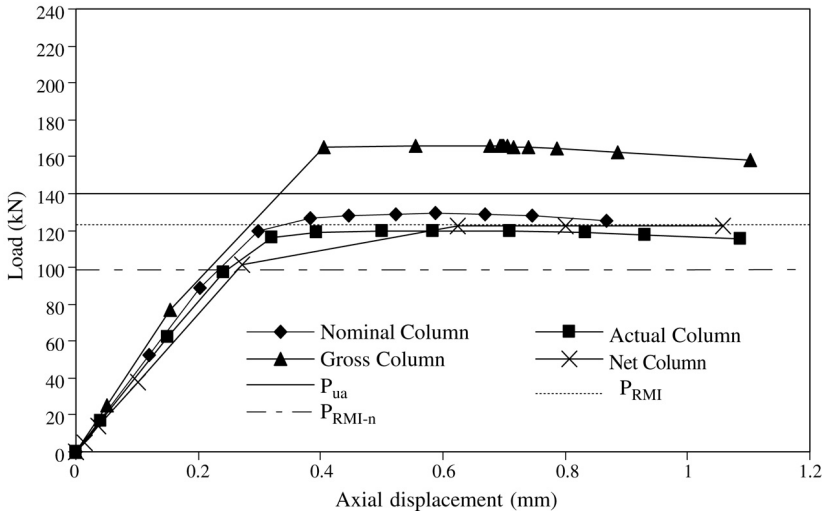

Fig. 7. Load versus displacement curves ($f_y = 250$ MPa).

– Cross section of the column without perforations, considering the area as the minimum net area of the column called *net column*.

Numerical analysis was carried out for nominal and experimental steel properties. These numerical results were compared with the experimental data (P_{ua}) and the RMI prescriptions values using experimental results to yielding stress as described in Section 3 (P_{RMI}) and using nominal values to yielding stress ($P_{RMI\text{-}n}$). The distortional buckling stress is not considered in RMI, but the rack cross section analyzed is controlled by this mode [13]. Figs. 7 and 8 represent graphically the applied load and the longitudinal displacement of the column, considering nominal and experimental material properties, respectively. It has been observed that the material properties have a strong influence on the results. It can be observed in Fig. 8 that all finite elements results were higher than the experimental ones. This can be justified by the use of yield stress (f_{ya}) from the stiffener wall, without perforations.

The representative curves of the nominal, net and actual columns indicate similar values to experimental data, varying from 8% to 17% from the average experimental ultimate loads. These curves have the same slope from the beginning up to the collapse load. When the nominal properties were considered, an approximation to RMI values could be observed. Table 3 presents the results for the ultimate loads, obtained by finite element analysis, which are compared with RMI and the experimental values. It can be seen that the simulation of the actual column is generally in good agreement with the experimental value ($P_{ua} = 139.73$ kN) and the RMI results using nominal and experimental material properties. It can be observed that the geometric imperfections influence the column strength.

From the simulation using the minimum net area emerges a possible alternative for a different design from the RMI procedure, which uses the experimental results of the

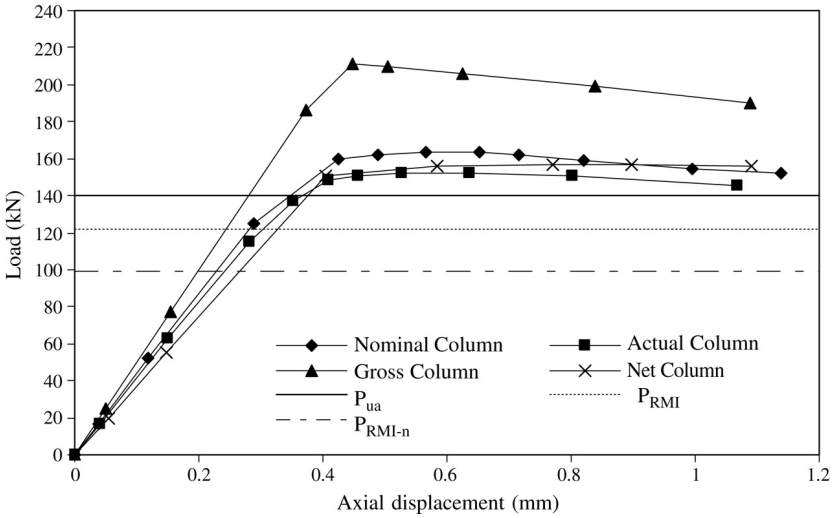

Fig. 8. Load versus displacement curves ($f_{ya} = 320.23$ MPa).

Table 3
Comparison between the experimental and the numerical ultimate load

Prototype	P_{ef} (kN)	P_{ef}/P_{ua}	P_{ef}/P_{RMI}	$P_{ef\text{-}n}$ (kN)	$P_{ef\text{-}n}/P_{RMI\text{-}n}$
Nominal Column	163.64	1.17	1.34	129.38	1.31
Actual Column	150.78	1.08	1.23	119.92	1.21
Gross Column	210.95	1.51	1.73	165.73	1.67
Net Column	156.57	1.12	1.28	122.48	1.24

$P_{ef\text{-}n}$—ultimate load obtained by finite element analysis with $f_y = 250$ MPa.
P_{ef}—ultimate load obtained by finite element analysis with $f_{ya} = 320.23$ MPa.
P_{ua}—experimental ultimate load (139.73 kN).
$P_{RMI\text{-}n}$—ultimate load obtained by RMI with $f_y = 250$ MPa (98.98 kN).
P_{RMI}—ultimate load obtained by RMI with $f_{ya} = 320.23$ MPa (122.14 kN).

stub columns in the design of the racks, since it is observed that the net column has good correlation with the experimental and RMI values.

5.3. Failure mode

The tests performed by Oliveira [4] show a horizontal displacement of the rear flanges in the middle of the height in the collapse mode, as illustrated in Fig. 9.

It is observed that in the case of the column without imperfections (Fig. 10(a)), a collapse mode opposes the experimental results (Fig. 9). The collapse mode was caused by the perforations of the cross section in the middle height of the column, which is the region of minimum area.

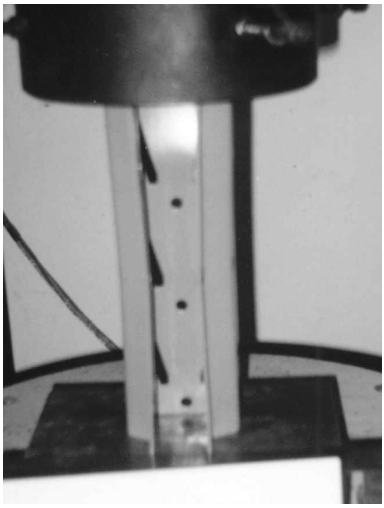

Fig. 9. Displacements in actual tests [4].

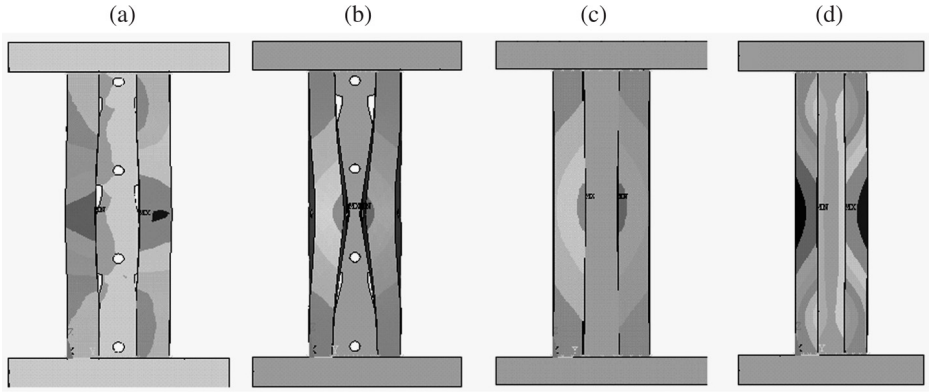

Fig. 10. Displacements in the simulations, with amplification factor of 10: (a) Nominal column; (b) Actual column; (c) Gross column; (d) Net column.

When the measured imperfections are included, Fig. 10(b), a collapse mode similar to the experimental one was observed, confirming the strong influence of the imperfections in stub columns.

For the cases where no perforations are observed the displacements in the middle height are smaller than in the other cases. The absence of perforations is thought to be responsible for this. During the tests local buckling of the web and the distortional mode were observed.

It is important to point out that for the numerical simulation of the gross column, nominal dimensions of the profile were considered. For the simulation of the net column

the minimum net area of the perforated section was used, maintaining the same width ratios between the plate elements.

6. Conclusions

A finite element analysis has been developed to study the influence of imperfections, perforations and material properties on the collapse mode and ultimate strength of rack cold-formed steel sections submitted to axial compression. In the model, shell, solid and contact finite elements were used to represent the stub column analyzed by the experimental program. The finite element model also used nominal and experimentally derived stress–strain relationships and geometric imperfection distribution. The finite element model considered different forms of cross-section areas and the results were compared with experimental results and code prescriptions. The comparison between test results and finite element results indicates good agreement of the ultimate load of the actual column and the net column. The comparison between code prescriptions (RMI) and finite element results indicates conservative values. When nominal yielding stress is used in finite element analysis the nominal column, actual column and net column indicated good agreement with experimental results. The model was also capable of predicting the local mode and distortional mode. The actual stub column specimen modeled by finite elements using the actual yield stress showed the best results of ultimate load and collapse mode compared to the other cross-section areas simulated.

Acknowledgements

The authors are grateful for the support from the Brazilian Council of Research and Development (CNPq- Edital Universal 01/2001-471550/01-9) and from private company Águia Sistemas de Armazenagem Industrial.

References

[1] Águia. Águia Sistemas de Armazenagem Industrial, catalogue, Ponta Grossa – PR; 1999 [in Portuguese].
[2] ANSYS User's Manual for revision 5.6. Swanson Analysis Systems Inc., Houston, PA; 1999.
[3] RMI. Specification for design, testing, and utilization of industrial steel storage racks. Charlotte (NC): Rack Manufacturers Institute; 1997.
[4] Oliveira AM. Theoretical-experimental analysis of industrial storage systems (Racks). M.Sc. diss., Ouro Preto (Minas Gerais, Brazil): Federal University of Ouro Preto; 2000 [in Portuguese].
[5] Freitas AMS, Ribeiro LFL, Oliveira AM. Theoretical-experimental analysis of Industrial storage racks systems. In: XXIX South American congress of structural engineering. 2000, CD-rom, p. 16 [in Portuguese].
[6] Hancock GJ. Design of cold-formed steel structures. 3rd ed. Sydney: Australian Institute of Steel Construction; 1998.
[7] AISI. Cold formed steel design manual. Washington (DC): American Iron and Steel Institute; 1996.
[8] Peköz T. Design of perforated cold formed steel columns. In: 9th international specialty conference on cold-formed steel structures. 1988.
[9] Abdel-Rahman N, Sivakumaran KS. Material properties models for analysis of cold-formed steel members. Journal of Structural Engineering 1997;123(9):1135–42.
[10] ASTM. E8M-95 A-Standard test methods for tension testing of metallic materials (Metric). American Society for Testing and Materials; 1995.

[11] Freitas AMS, Freitas MSR, Oliveira AM, Cabral JB, Souza FT. Theoretical-experimental analysis of perforated cold-formed metallic columns. In: I international congress on steel construction (I CICOM). 2001, CD-rom, p. 12 [in Portuguese].
[12] Freitas MSR, Freitas AMS, Souza FT. Analysis of cold formed steel columns through the finite element method. In: V Simpósio Mineiro de Mecânica Computacional. 2002, p. 17–24 [in Portuguese].
[13] ABNT NBR-14672. Dimensionamento de Estruturas de Aço Constituídas por Perfis Formados a Frio. 2001 [in Portuguese].